A Novel, Sensitive Potentiometric Hydrocarbon Sensor for High-Vacuum Applications

Georgios Kyriakou,[†] David J. Davis,[†] Robert B. Grant,[‡] Mintcho S. Tikhov,[†] Anthony Keen,[‡] Philip Pakianathan,[‡] and Richard M. Lambert*,[†]

Chemistry Department, Cambridge University, Cambridge CB2 1EW, England, and Lithography Subsystems, BOC Edwards, Manor Royal, Crawley, West Sussex, United Kingdom

Received: July 21, 2006; In Final Form: September 27, 2006

A potentiometric device based on interfacing a solid electrolyte oxygen ion conductor with a thin platinum film acts as a robust, reproducible sensor for the detection of hydrocarbons in high- or ultrahigh-vacuum environments. Sensitivities in the order of $\sim 5 \times 10^{-10}$ mbar are achievable under open circuit conditions, with good selectivity for discrimination between *n*-butane on one hand and toluene, *n*-octane, *n*-hexane, and 1-butene on the other hand. The sensor's sensitivity may be tuned by operating under constant current (closed circuit) conditions; injection of anodic current is also a very effective means of restoring a clean sensing surface at any desired point. XPS data and potentiometric measurements confirm the proposed mode of sensing action: the steady-state coverage of O_a, which sets the potential of the Pt sensing electrode, is determined by the partial pressure and dissociative sticking probability of the impinging hydrocarbon. The principles established here provide the basis for a viable, inherently flexible, and promising means for the sensitive and selective detection of hydrocarbons under demanding conditions.

Introduction

Surface contamination of critical components by adsorption of organic molecules can seriously compromise the integrity of costly high-vacuum-process technologies, for example, in the semiconductor device fabrication industry. For example, adventitious hydrocarbon species, when present at pressures lower than 10^{-6} mbar, can seriously degrade the reflectivity of the multilayer mirrors proposed for use in extreme ultraviolet (EUV) lithography, an important next generation technology.[1,2] Similar contamination issues arise in high-vacuum-based electron lithographic processes. Process control in such systems would be therefore greatly enhanced by the availability of high-vacuum-compatible, compact, low-cost, robust, selective hydrocarbon sensors for point-of-use applications whereby many such sensors could be deployed at key points to detect contamination events so as to protect sensitive and costly equipment.[3−5] In this regard, it is important to note that some hydrocarbons are harmful whereas others are benign—so in terms of sensing, selectivity is as important as sensitivity.

It has been proposed[5] that an oxygen ion conducting solid electrolyte (yttria-stabilized zirconia, YSZ) when interfaced with platinum sensing and reference electrodes could be operated as a potentiometric sensor for hydrocarbons under ultrahigh-vacuum conditions—the oxygen activity at the sensing electrode being determined by the hydrocarbon partial pressure. Previously[3] by means of XPS and temperature-programmed reaction measurements we demonstrated the suitability of polycrystalline platinum as a sensing electrode for sensitive and selective detection of hydrocarbons in a vacuum environment by electrochemical means. At 870 K (anticipated temperature for sensor operation) all the species investigated underwent precursor-mediated dissociative adsorption to yield graphite, though at widely different rates. It was found that polycrystalline platinum discriminated effectively between "sticky" hydrocarbons such as alkenes, aromatics, and alkanes > C_5 on one hand, and "benign" low molecular weight alkanes on the other. Subsequently,[4] we showed that polycrystalline, gold-rich Au/Pt bimetallic surfaces are very promising for use as sensitive and *selective* hydrocarbon sensing electrodes: by adjusting the surface composition, they may be used to discriminate, variously, between alkanes, alkenes, and aromatics.

Here we report the first successful implementation of the proposed concept.[5] A sensitive potentiometric hydrocarbon sensor has been built and operated under conditions directly relevant to the intended application. Working with five different hydrocarbons and by means of in situ XPS and potentiometric measurements, fundamental information about the mode of sensor action has also been obtained.

Experimental Section

Figure 1 shows a photograph of the sensor, a 3D representation of the sensor body, and a schematic of the sensing head. The sensor consisted of an 8 mol % YSZ tube (FRIATEC AG) one end of which was closed; this was interfaced with a ~ 7 cm^2 external Pt film (W) ~ 1 μm thick with an active surface area[6] of ~ 200 cm^2 that served as the working (sensing) electrode, and a ~ 7 cm^2 internal Pt film (C) that served as the counter electrode. A small Au reference electrode (R) was also located on the inner wall of the YSZ tube, all electrodes being deposited by DC sputtering. The outside of the YSZ tube was immersed in the UHV environment whose gas composition was to be analyzed while the inner (reference) compartment was maintained at atmospheric pressure by circulating air through it. The sensor assembly could be translated and rotated within the UHV chamber so as to optimize its position for XPS measurements. The YSZ tube was heated to operating temperature ($\sim$873 K) by an electrically insulated coil located against the inner wall of the YSZ tube and two K-type thermocouples

* Address correspondence to this author. Fax: +44 (0)1223 336362. Phone: +44 (0)1223 336467. E-mail: rml1@cam.ac.uk.
[†] Cambridge University.
[‡] Lithography Subsystems, BOC Edwards.

10.1021/jp064635h CCC: $33.50
Published on Web 11/07/2006

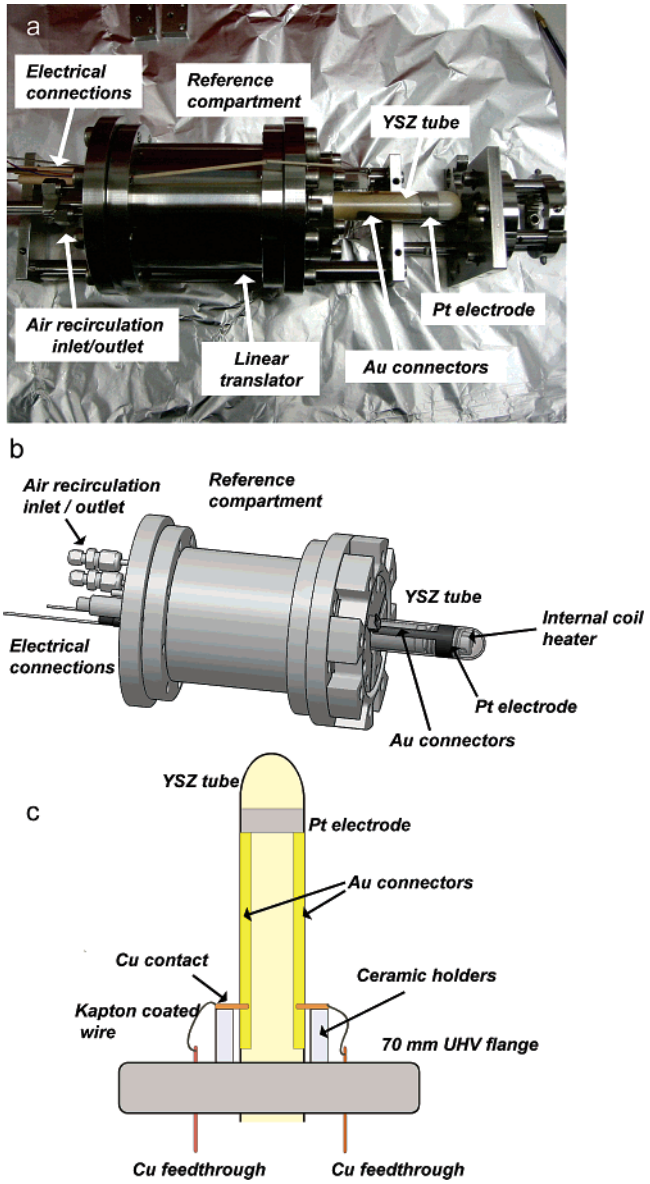

Figure 1. (a) Picture of the sensor on the linear translator; (b) 3D schematic of the sensor body; and (c) diagram of the sensing head.

were used to monitor temperature at the surface of the working (sensing) electrode and within the reference compartment.

Measurements were carried out in a UHV chamber operated at a base pressure of 3×10^{-9} mbar and described in detail elsewhere.[7] It was equipped with a VSW100 hemispherical analyzer, a dual (Mg/Al) X-ray source, and a VG SensorLab quadrupole mass spectrometer whose ionizer could be located 60 mm from the working (sensing) electrode. The surface composition of the sensing electrode was monitored by XPS, and the electrode was electrochemically cleaned by applying an anodic current at 883 K so as to combust surface carbon present on the Pt surface by supplying oxygen from the reference side. XP spectra were collected by using Mg Kα radiation with the working electrode grounded. *n*-Hexane (99+%), toluene (99.8%), and *n*-octane (99+%) were obtained from Sigma-Aldrich while 1-butene (99.9%) and *n*-butane were obtained from BOC special gases. All pressures quoted here have been corrected for molecular ionization cross sections. Potentiometric measurements (under both open circuit and galvanostatic conditions) were carried out by means of two source meters (Keithley 2400) interfaced with a computer: this allowed simultaneous monitoring of the working/counter (V_{WC}) and working/reference (V_{WR}) electrode potential differences.

Results and Discussion

Behavior in the Absence of Deliberately Added Hydrocarbons. Whatever the initial state of the working electrode, allowing the sensor to equilibrate under open circuit conditions at a temperature of 883 K and with a base pressure of 3×10^{-9} mbar in the UHV compartment always eventually resulted in a carbon-free, oxygen-containing working electrode (XPS) with V_{WR} and V_{WC} ca. -0.5 and -0.4 V, respectively. This is the result of spontaneous oxygen semipermeation[8,9] to the working electrode resulting in burn-off of carbonaceous species. (Open circuit oxygen transport from the reference compartment to the UHV side occurs spontaneously because YSZ, at high temperatures and under large oxygen partial pressure differences between the sampling and reference side, exhibits some electronic conductivity.[7,8]) This property of the system was actually beneficial because it provided an in-built recovery mechanism for clean-off of the working electrode after operation in the sensing mode.

When constant **cathodic** currents (I_{WC}) were imposed between the working and counter electrodes (electropumping oxygen **away** from the working electrode), the potential of the working electrode (V_{WR}) decreased, as expected. Figure 2a depicts the time dependence of V_{WR} starting with open circuit conditions, then during imposition of $I_{WC} = -10$ μA followed by a period at $I_{WC} = -20$ μA, then open circuit again. It can be seen that switching on $I_{WC} = -10$ μA causes V_{WR} to reach a new steady-state value of ca. -1.2 V; increasing I_{WC} to -20 μA causes a further decrease in V_{WR} to a new steady-state value of ca. -1.4 V. Finally, returning to open circuit conditions resulted in a slow rise in V_{WR}, which eventually returned to its initial value of ca. -0.5 V after $\sim$24 h: this is an illustration of the oxygen semipermeation effect described above.

Figure 2b shows O 1s XP spectra acquired simultaneously with the data in Figure 2a corresponding to the $I_{WC} = -10$ μA region shown in Figure 2a. Spectrum **a** in Figure 2b shows the O 1s emission from the sensing electrode under *open circuit equilibrium conditions*. It consists of a broad feature that can be fitted with the following components: **B** centered at 530.4 eV, which corresponds to chemisorbed adatoms;[10] **C** centered at 531.8 eV, which corresponds to platinum oxide;[11] and **A** centered at 529.5 eV, which has been reported by others[12,13] and is assigned to an ionic backspillover species [13] or to subsurface oxygen.[12] As we shall see, in the present context species **A** is not of prime importance: it disappeared as soon as any cathodic current was applied. (Oxygen in the underlying YSZ was XPS invisible due to the thickness of the Pt film and the near-normal exit photoelectron detection geometry.)

Spectra **b**, **c**, and **d** were recorded consecutively during application of a cathodic current ($I_{WC} = -10$ μA) and the corresponding integrated intensities (arrowed) are plotted, along with others, in Figure 2a. The XPS data acquisition time was $\sim$2 min, which is relatively short compared to the time scale of the experiment ($\sim$66 min). Component **A** disappeared rapidly, while **B** diminished more slowly. The intensity of the oxidic oxygen **C** initially decreased and then remained unchanged for the rest of the experiment. We interpret these observations as follows: chemisorbed oxygen (**B**) is the species that determines the potential of the electrode according to

$$O^{2-}(YSZ) \rightarrow O_a(Pt) + 2e^-$$

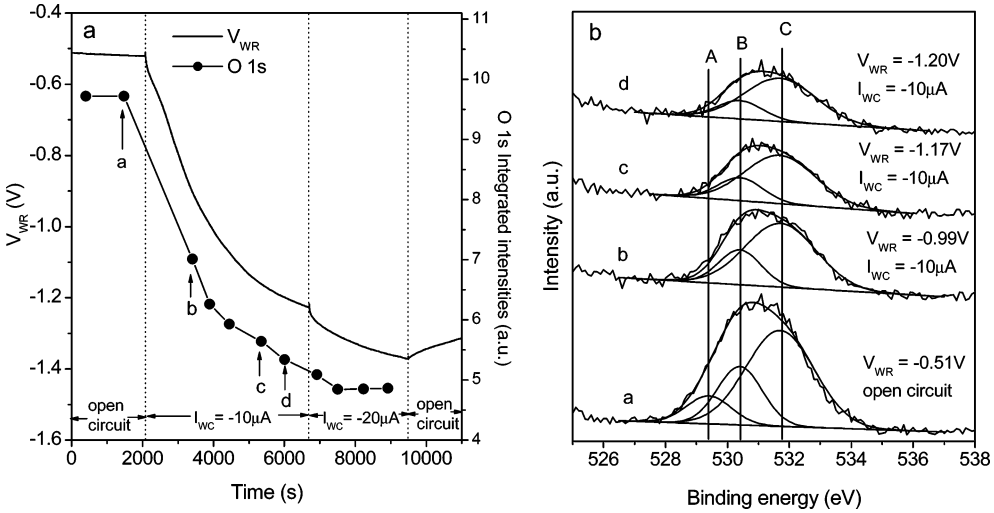

Figure 2. (a) V_{WR} and O 1s variation upon passing cathodic I_{WC} currents. (b) O 1s XP spectra for constant cathodic I_{WC} currents.

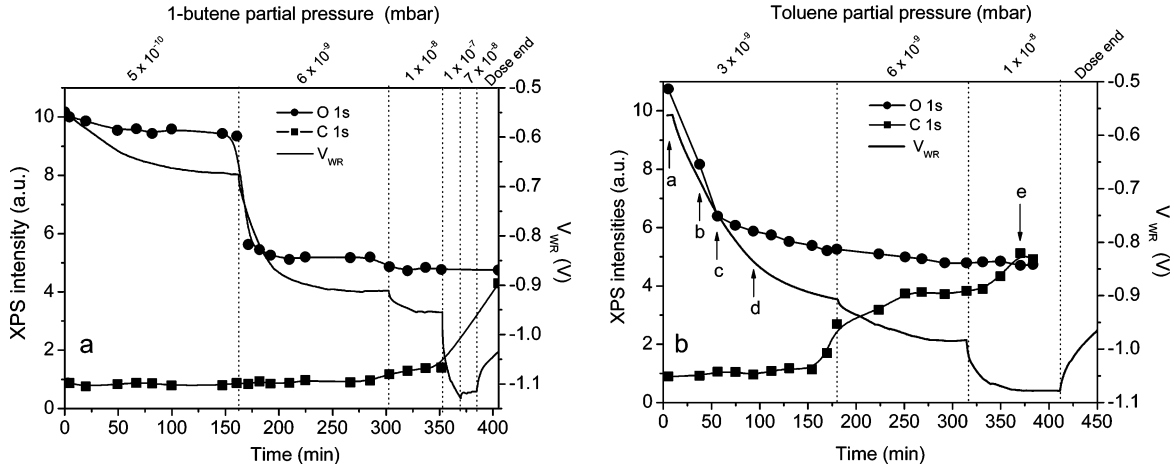

Figure 3. V_{WR} response to (a) 1-butene and (b) toluene as a function of pressure and time. Data are presented alongside the C 1s and O 1s integrated intensities.

Under sensing conditions (i.e. deliberately added hydrocarbon) the surface concentration of O_a, and hence the value of V_{WR}, depends on the rate of deposition of carbon and hence on the hydrocarbon partial pressure (a simple analysis is given in Appendix I). The remaining "oxidic" component **C** corresponds to a small amount of oxygen dissolved in the Pt: this oxygen, distributed throughout the thin film, plays no role in the chemistry. It is XPS visible because the O 1s kinetic energy (722 eV) corresponds to a sampling depth of 1.4 nm.

Operating Modes. The sensor could be operated in any of three modes that were capable of providing information about the presence of nonbenign hydrocarbons at very low pressure levels. These modes correspond to open circuit, constant current or constant potential. The first two fall into the category of solid electrolyte potentiometry; the third is often referred to as amperometric sensing. Here we shall focus on potentiometric sensing. Amperometric sensing will be the subject of a separate report.

Open Circuit Mode. Panels a and b of Figure 3 illustrate the *open circuit response* (V_{WR}) of the sensor to increasing partial pressures of 1-butene and toluene, respectively; the corresponding O 1s and C 1s integrated intensities are also shown. It is clear that there is a pronounced response, even at hydrocarbon pressures of $\sim 3 \times 10^{-10}$ mbar. After each increase in hydrocarbon partial pressure V_{WR} decreased and attained a new steady state value. In the steady state, the rate of oxygen removal by reaction with carbonaceous species at the catalytically active Pt working electrode is equal to the rate of oxygen delivery by semipermeation from the reference side. At the end of the sequence, when the hydrocarbon feed was shut off, V_{WR} recovered slowly as oxygen semipermeation burned off the deposited carbonaceous species. (We shall see later that the recovery process can be greatly accelerated by deliberately electropumping oxygen to the working electrode.)

The simultaneously acquired XP C 1s and O 1s spectra provide important confirmation of the proposed mode of sensing action. Consider Figure 3a. When the 1-butene pressure was increased from 6×10^{-9} to 1×10^{-8} mbar, the drop in V_{WR} was accompanied by a decrease in the O 1s intensity and a small but detectable increase in C 1s intensity. Successive increases in 1-butene pressure resulted in further decreases (increases) in the O 1s (C 1s) intensities. At low adsorbate coverages, XPS is much less sensitive than V_{WR} because the latter depends logarithmically on the hydrocarbon pressure (see text below, Figure 6, and Appendix I). Note that at the highest hydrocarbon pressure there is a large increase in the C 1s intensity reflecting high steady state carbon coverage in the presence of the limited supply of oxygen from semipermeation. The toluene data in Figure 3b exhibit essentially the same characteristics: carbon accumulation is similar to 1-butene, due to the high dissociative sticking probability of both molecules on Pt under these conditions, as previously shown.[3] The behavior illustrated in Figure 3 was stable and fully reproducible: in the case shown,

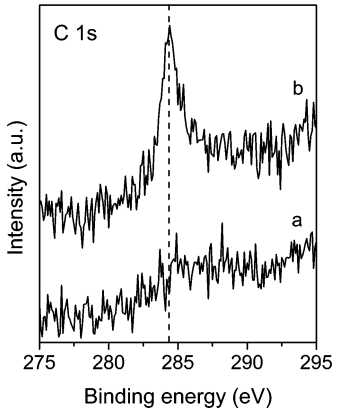

Figure 4. In situ C 1s spectra after exposing the sensor to toluene for 370 min as shown in Figure 3b.

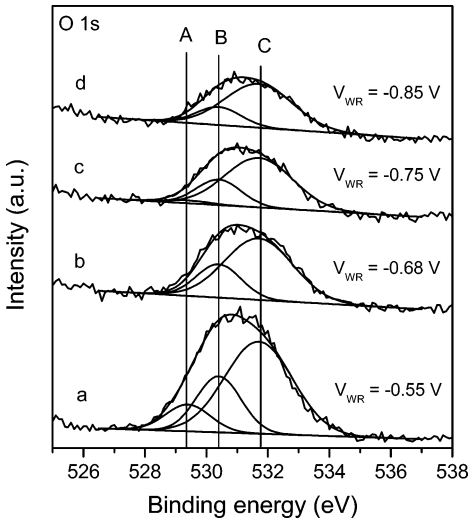

Figure 5. In situ O 1s spectra while exposing the sensor to toluene as shown in Figure 3b at (a) $t = 0$ min; (b) $t = 38$ min; (c) $t = 55$ min; and (d) $t = 95$ min.

the experiments were repeated three times and produced essentially identical data.

The C 1s spectrum shown in Figure 4 corresponds to a toluene exposure time of ~370 min (arrowed with **e** in Figure 3b). It consists of a single peak, centered at 284.4 eV, which can confidently be assigned to graphitic carbon.[3,14−16] This agrees well with our earlier study on a polycrystalline Pt model electrode where the adsorption of toluene, 1-butene and various other hydrocarbons at 870 K always produced a graphitic deposit.[3] The time evolution of the O 1s spectra whose integrated intensities (arrowed with **a**−**d**) are plotted in Figure 3b is illustrated in Figure 5. Species **A** disappeared quickly after introduction of the hydrocarbon. The "oxidic" species **C** initially decreased and then remained essentially constant. The chemisorbed oxygen (species **B**) was steadily consumed by reaction with deposited carbon, disappearing completely at $V_{WR} \approx -0.9$ V (spectrum not shown) consistent with the proposed mode of sensing action: by the time steady state is reached the key chemically active species that sets the value of V_{WR} and whose concentration depends on the hydrocarbon partial pressure is O_a.

According to the simple analysis presented in Appendix I, V_{WR} is expected to vary as the logarithm of the hydrocarbon partial pressure. Figure 6 shows the observed variation of V_{WR} with partial pressure for 1-butene, toluene, *n*-butane, *n*-hexane, and *n*-octane. Over most of the range explored, it is evident

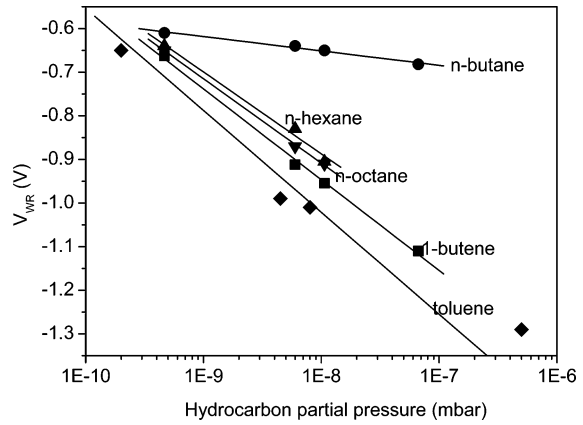

Figure 6. V_{WR} change as a function of hydrocarbon partial pressure for toluene, 1-butene, *n*-octane, *n*-hexane, and *n*-butane.

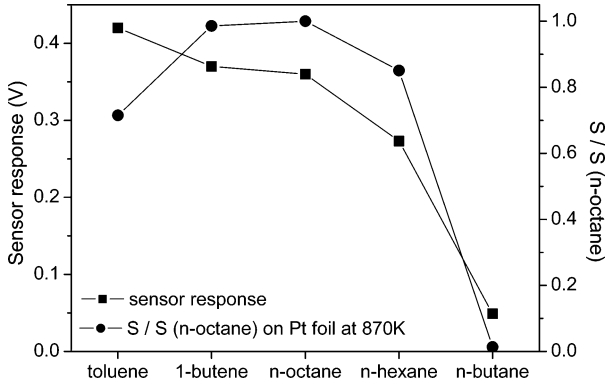

Figure 7. Left axis: Sensor response to 6×10^{-9} mbar of toluene, 1-butene, *n*-octane, *n*-hexane, and *n*-butane. Right axis: Relative sticking coefficient of the same hydrocarbons on a Pt polycrystalline foil at 870 K as calculated in ref 3.

that the V_{WR} does indeed vary linearly with the logarithm of hydrocarbon partial pressure. Small deviations from linearity are apparent when the hydrocarbon pressure rose above the point at which the buildup of graphitic carbon on the working electrode became substantial (XPS). A possible explanation is that under these conditions $[O_a]$ is controlled by mass transport effects rather than the rate of reaction with the graphitic deposit. It is clearly evident from Figure 6 that the sensor response is dependent on hydrocarbon functionality. In particular, the response of the sensor to the benign hydrocarbon *n*-butane is very different from its response to all the other "stickier" hydrocarbons. Toluene produces the strongest response followed by 1-butene; the alkanes produce responses that decrease with decreasing chain length. These data are in very good quantitative agreement with our earlier work in which we investigated the suitability of polycrystalline Pt foil as a model working electrode for hydrocarbon sensing applications.[3] The observed trends in rates of graphitic carbon accumulation were understandable in terms of the sticking coefficients for dissociative adsorption of the various hydrocarbon species; here we confirm that this parameter does indeed determine the sensor's response. Thus Figure 7 shows a plot of the sensor response to 6×10^{-9} mbar of each of toluene, 1-butene, *n*-octane, *n*-hexane, and *n*-butane. Also shown are the relative sticking probabilities of these hydrocarbons as calculated from our previous work on polycrystalline Pt foil.[3] (Sensor response is defined as $\Delta V^{o}_{WR} = V^{i}_{WR} - V^{f}_{WR}$, where V^{i}_{WR} and V^{f}_{WR} are the initial and final steady-state values, respectively, of V_{WR} before and after admitting 6×10^{-9} mbar of each hydrocarbon to the UHV

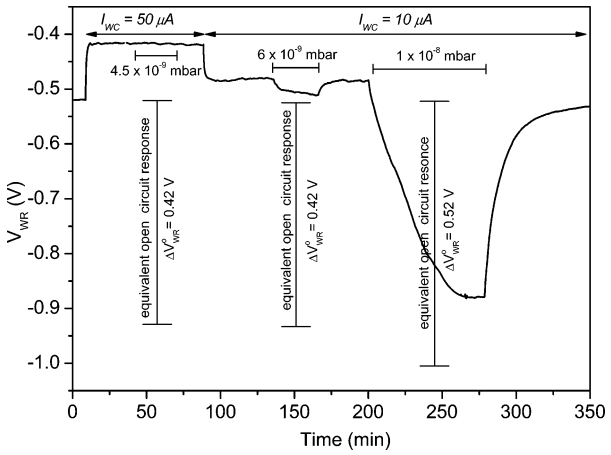

Figure 8. V_{WR} response to different toluene partial pressures under constant current operation of the sensor. The respective open circuit sensor responses, ΔV^o_{WR}, to the same toluene partial pressures are also shown.

chamber.) It can be seen that the correlation between the two properties is quite good.

Sensing in Constant Current Mode. The preceding data demonstrate that open circuit measurements can be used to monitor reliably very low hydrocarbon levels in UHV systems with a good degree of selectivity between *n*-butane and the rest of the molecules. We now show that the dynamic range and speed of response can be improved at the expense of sensitivity by operating in constant current mode. In this mode, a constant current, I_{WC}, is passed between the working and counter electrodes, which, depending on the polarity, imposes a constant rate of supply or removal of oxygen to or from the working electrode. Then, upon hydrocarbon admission, V_{WR} changes by an amount that is determined by (i) the partial pressure of the hydrocarbon and (ii) the magnitude of I_{WC}, which provides independent control of the oxygen flux at the working electrode.

Figure 8 illustrates the characteristics of the sensor when operated in constant current mode. After an initial period under open circuit conditions, at $t = 10$ min a constant anodic current (oxygen pumped *to* the working electrode) $I_{WC} = 50$ μA was imposed, which introduced an overpotential of 0.1 V. Admission of 6×10^{-9} mbar of toluene at $t = 40$ min produced a negligible response. This is to be compared with Figure 3 where the corresponding open circuit response was -0.98 V; this open circuit response is also indicated in Figure 8. This is because electrochemically supplied oxygen produces a much higher steady-state coverage of O_a compared to that produced by semipermeation under open circuit conditions. As a result, for a given hydrocarbon pressure, the change in O_a coverage (and hence the change in V_{WR}) due to carbon combustion is much smaller than it is under open circuit conditions. Reducing I_{WC} to 10 μA at $t = 90$ min reduced the overpotential to 0.03 V and substantially increased sensitivity, as would be expected on the basis of the above argument: lower steady-state oxygen coverage undergoes greater relative decrease for a given hydrocarbon pressure. Note that at 1×10^{-8} mbar the response is much larger—approaching the open circuit response: V_{WR} responds approximately logarithmically to the change in hydrocarbon pressure. Thus current injection may be used to tune the sensitivity of the device. Note that even if maximum sensitivity is required (open circuit operation) rapid recovery of the sensor to its initial state can readily be achieved by briefly imposing an anodic current to burn off accumulated carbon: 50 μA restores the initial (clean) value of V_{WR} in seconds.

In light of these encouraging results, further work is planned in which sensor selectivity will be tuned by application of bimetallic working electrodes, ultimately implemented in arrays in which the elements have overlapping but different selectivity profiles. The outputs from such a device should be suitable for processing by application of fuzzy logic and artificial neural networks, enabling even greater chemical selectivity to be achieved.

Conclusions

1. Solid electrolyte potentiometry provides a viable, inherently flexible, and promising means for the sensitive detection of hydrocarbons in high- or ultrahigh-vacuum environments.
2. Platinum is an effective material for use as the working electrode, providing excellent reproducibility and a degree of selectivity between benign and harmful hydrocarbons. (Alloying with Au is expected to substantially enhance selectivity).
3. Sensitivities in the 5×10^{-10} mbar range are achievable under open circuit operation.
4. Sensitivity may be tuned by operating under constant current conditions; current injection is also a very effective means of restoring a clean sensing surface.
5. XPS data in combination with potentiometric measurements provide confirmation of the proposed mode of sensing action: the steady-state coverage of O_a, which sets V_{WR}, is determined by the partial pressure and dissociative sticking probability of the impinging hydrocarbon.

Acknowledgment. G.K., D.J.D., and M.S.T. acknowledge financial support from BOC Edwards. D.J.D. acknowledges a research studentship awarded by the UK Engineering and Physical Sciences Research Council.

Appendix 1

By following a similar analysis to the one presented by Fleming[17] for mixed potential CO gas sensors, the presence of hydrocarbons on the working side of the sensor can affect the open circuit voltage by either direct or indirect participation in the electrochemical reaction:

(i) *Indirect participation* of the hydrocarbon in the electrochemical reaction can take place due to the following reaction:

$$C_xH_y + \left(2x + \frac{y}{2}\right)O_{(a)}(Pt) \rightarrow xCO_2 + \frac{y}{2}H_2O \qquad (1)$$

In this case the electrochemical reaction that determines the open circuit sensor voltage is

$$O_2 + 4e^- \leftrightarrow 2O^{2-} \qquad (2)$$

The oxygen at the working electrode is provided by spontaneous semipermeation due to the extreme pressure difference between the working and the reference side (see text and references). The arriving oxygen ions on the working electrode are converted to oxygen adatoms by the following net-charge reaction in the three-phase boundary:

$$O^{2-} \leftrightarrow O_{(a)}(Pt) + 2e^- \qquad (3)$$

In this case the galvanic cell is defined as

$$P_{O_2}(\text{ref}),\text{Au}|\text{YSZ}|\text{Pt},P_{O_2}(\text{working}) \qquad (4)$$

and the sensor voltage can be determined by Nernst's equation:

$$V = V^{o}_{O_2} + \frac{RT}{4F}\ln\left(\frac{P^{W}_{O_2}}{P^{R}_{O_2}}\right) \quad (5)$$

If one assumes a Langmuir−Hinshelwood type reaction between the hydrocarbon and O_a(Pt) then the hydrocarbon partial pressure is expected to be inversely proportional to the amount of O(a) and therefore the sensor voltage would vary logarithmically with the hydrocarbon partial pressure as observed.

(ii) *Direct participation* of the hydrocarbon in the electrochemical reaction can take place by the reaction of the hydrocarbon with O^{2-} at the three-phase boundary that will introduce a mixed potential:

$$C_xH_y + \left(2x + \frac{y}{2}\right)O^{2-} \rightarrow xCO_2 + \frac{y}{2}H_2O + (4x + y)e^{-} \quad (6)$$

In this case the galvanic cell is defined as

$$P_{O_2}(\text{ref}),\text{Au}|\text{YSZ}|\text{Pt},P_{C_xH_y}(\text{working}) \quad (7)$$

and the open circuit voltage due to the hydrocarbon is determined by

$$V_{C_xH_y} = V^{o}_{C_xH_y} + \frac{RT}{(4x + y)F}\ln\left(\frac{(P^{W}_{CO_2})^{x}(P^{W}_{H_2O})^{y/2}}{(P^{R}_{O_2})^{(x+y/4)}(P^{W}_{C_xH_y})}\right) \quad (8)$$

Finally if one assumes that the cell output voltage depends on the existence of both reactions 2 and 7 on the working electrode then the open circuit voltage will depend on both V_{O_2} and $V_{C_xH_y}$:

$$V = \theta_{O_2}V_{O_2} + \theta_{C_xH_y}V_{C_xH_y} \quad (9)$$

where θ_{O_2} and $\theta_{C_xH_y}$ are the fractional coverage of oxygen and hydrocarbon on the working electrode surface. By combining then eqs 5, 8, and 9 an expression for the open circuit voltage can be obtained:

$$V = \theta_{O_2}\left[V^{o}_{O_2} + \frac{RT}{4F}\ln\left(\frac{P^{W}_{O_2}}{P^{R}_{O_2}}\right)\right] + \theta_{C_xH_y}\left\{V^{o}_{C_xH_y} + \frac{RT}{(4x + y)F}\ln\left[\frac{(P^{W}_{CO_2})^{x}(P^{W}_{H_2O})^{y/2}}{(P^{R}_{O_2})^{(x+y/4)}(P^{W}_{C_xH_y})}\right]\right\} \quad (10)$$

References and Notes

(1) Kurt, R.; van Beek, M.; Crombeen, C.; Zalm, P.; Tamminga, Y. *Proc. SPIE* **2002**, *4688*, 702.

(2) Mertens, B.; et al. *Microelectron. Eng.* **2004**, *73*−*74*, 16.

(3) Kyriakou, G.; Davis, D. J.; Lambert, R. M. *Sens. Actuators, B* **2006**, *114*, 1013.

(4) Davis, D. J.; Kyriakou G.; Lambert R. M. *J. Phys. Chem. B* **2006**, *110*, *11958*.

(5) Grant, R. B. International Patent, WO 2005/019817 A1.

(6) Yentekakis, I. V.; Palermo, A.; Filkin, N. C.; Tikhov, M. S.; Lambert, R. M. *J. Phys. Chem. B* **1997**, *101*, 3759.

(7) Horton, J. H.; Moggridge, G. D.; Ormerod, R. M.; Kolobov, A. V.; Lambert, R. M. *Thin Solid Films* **1994**, *237*, 134.

(8) Sridhar, K. R.; Blanchard, J. A. *Sens. Actuators, B* **1999**, *59*, 60.

(9) Fujiwara, Y.; Kaimai, A.; Hong, J.; Yashiro, K.; Nigara, Y.; Kawada, T.; Mizusaki, J. *J. Electrochem. Soc.* **2003**, *150*, E117.

(10) Luerâen B.; Janek, J.; Imbihl R. *Solid State Ionics* **1997**, *93*, 263

(11) Aita, C. R.; Tran, N. C. *J. Appl. Phys.* **1984**, *56*, 958.

(12) Reinhartd, G.; Mayer, R.; Rösch, M. *Solid State Ionics* **2002**, *150*, 79.

(13) Vayenas, C. G.; Lambert, R. M.; Ladas, S.; Bebelis, S.; Neophytides, S.; Tikhov, M. S.; Filking N. C.; Makri M.; Tsilpakides, D.; Cavalca C.; Besocke, K. *Stud. Surf. Sci. Catal.* **1997**, *112*, 39.

(14) Ranke, W.; Weiss, W. *Surf. Sci.* **2000**, *465*, 317.

(15) Paal, Z.; Schlögl, R.; Ertl, G. *J. Chem. Soc., Faraday Trans.* **1992**, *88*, 1179.

(16) Weckhuysen, B. M.; Rosynek, M. P.; Lunsford, J. H. *Catal. Lett.* **1998**, *52*, 31.

(17) Fleming, W. J. *J. Electrochem. Soc.* **1977**, *124*, 21.